Pergamon

Computers Math. Applic. Vol. 27, No. 8, pp. 101–117, 1994

0898-1221/94 $7.00 + 0.00

0898-1221(94)E0039-M

Recognizing Cylindrical Objects by Single Camera Views

C. H. LIU
Institute of Computer Science and Information Engineering
National Chiao Tung University, Hsinchu, Taiwan 300, R.O.C.

W. H. TSAI*
Department of Computer and Information Science
National Chiao Tung University, Hsinchu, Taiwan 300, R.O.C.

(Received and accepted January 1993)

Abstract—A new approach to recognition of cylindrical objects by single camera views using camera calibration, surface backprojection, and model matching techniques is proposed. Cylindrical objects to be recognized can be of different radii and heights. Both the silhouette shapes and the surface patterns of objects are utilized in the recognition scheme. A new camera calibration technique is first employed to compute the camera parameters analytically using a single camera view of the object. A surface backprojection technique is then adopted to reconstruct the pattern on the surface patch of the input object. The reconstructed surface pattern is finally matched with that of each object model, using a partial shape matching technique to find the best matching surface patch pattern of the models, from which the input object is classified accordingly. Experimental results showing the feasibility of the proposed approach are also included.

Keywords—Object recognition, Camera calibration, Surface backprojection, Model matching, Surface patterns, Partial shape matching.

1. INTRODUCTION

It is often found necessary to recognize 3-D objects in industrial automation. Among the 3-D objects, cylindrical objects (e.g., cans) appear frequently. Very few existing 3-D object recognition systems recognize cylindrical objects. And most related works focus on recognizing 3-D objects using silhouette shape information only; object surface patterns such as special marks or characters are less utilized. In this study, it is desired to use both the silhouette shapes and the surface patterns of 3-D objects to achieve better recognition results.

Chin and Dyer [1] presented a good survey of model-based computer vision works. Besl and Jain [2] discussed 3-D object recognition problems and a lot of 3-D object recognition systems were reviewed. Many new 3-D recognition systems were proposed in recent years. But few of them resembled the proposed approach. Since it is impossible to review all existing systems, only those with their recognition methods closer to the proposed approach are reviewed here.

Silberberg *et al.* [3] used the generalized Hough transform technique to match input 2-D line segments and edge junctions with 3-D model line segments and vertices. For each pair of line segments being matched, the model line is projected onto the image line, and the corresponding cell in the Hough accumulator array is incremented if the matching is successful.

This work is partially supported by the National Science Council, Republic of China, under Contract Number NSC 82-0404-E-009-157.
*Author to whom all correspondence should be sent.

Wang *et al.* [4] recognized 3-D objects by 2-D silhouette shapes. Each object model consists of the three principal axes, the principal moments, and the Fourier descriptors of the silhouette shape boundaries as viewed from the three principal axes. To recognize an input object, at least three silhouette views from distinct directions should be taken. Silhouette boundaries are then combined to produce an object from which the moments and the Fourier descriptors can be computed and matched against the model library.

Wallace and Wintz [5] used the Fourier descriptors of 2-D silhouette shapes to recognize 3-D aircraft. A library of 2-D shape descriptors for all discrete viewing directions covering the entire spherical solid angle is created. Recognition is accomplished by matching input shape descriptors against all the data in the library. Similar techniques were also used by Dudani *et al.* [6].

Watson and Shapiro [7] matched 2-D perspective views of 3-D objects with object models consisting of closed connected curved edges of the objects. Input 2-D scenes are processed to extract curves which are also described by Fourier descriptors. Object recognition is accomplished by comparing the 2-D perspective projections of the model curve with the input curve after the former is properly rotated and translated.

Liu and Tsai [8] proposed a 3-D curved object recognition system including a turn-table, a top-view camera, and a lateral-view camera. A 3-D object was recognized by first normalizing the orientation and position of the top-view silhouette shape by its principal axis and centroid, and then matching the shape features of the 2-D silhouette shapes of the input object against those of each object model by traversing a decision tree. Yang and Tsai [9] used 2-D cross-sectional slice shapes, instead of 2-D silhouette shapes, to recognize 3-D objects in a similar way.

In the previously-mentioned approaches, a common property is that input 3-D objects are recognized by matching processed input object images or representations against 2-D reference object models. This type of approach may be said to be 3-D recognition by 2-D matching. An advantage of this type of approach is that well-developed 2-D image analysis techniques can be utilized. However, a shortcoming is that extra effort must be paid to avoid exhaustive matching of input 2-D data with essentially an infinite number of possible views of each 3-D reference object.

Aside from the above type of approach, another contrastive type is 3-D recognition by 3-D matching, i.e., to recognize 3-D objects by matching 3-D input object data with 3-D object models. In approaches of this type, it is usually required to acquire 3-D object surface data and to transform them into certain 3-D representations, such as attributed hypergraphs [10], relational feature graphs [11], generalized cylinders [12], etc., before the final recognition step can be performed. But such 3-D data acquisition and modeling works usually take long computation time and cause 3-D recognition by 3-D matching inapplicable in many applications.

In this paper, we propose a new approach to 3-D object recognition which is basically a combination of the above two types of approaches but without their disadvantages. Objects to be recognized are assumed to have cylindrical shapes. The proposed approach consists mainly of three steps:

(1) 3-D object surface data acquisition by a new camera calibration technique;
(2) reconstruction of 2-D patterns on object surface patches by a backprojection technique; and
(3) model matching using 2-D patterns on surface patches for object recognition.

In the first step, the side lines and the bottom curve on the object surface in an object image is extracted, and the camera parameters are computed in an on-line fashion using a set of analytical formulas derived in this study. A backprojection technique used in computer graphics is then employed in the second step, to compute the 3-D pixel data of each surface patch appearing in the input object image and to transform the 3-D data into 2-D patterns. In the final step, the 2-D patterns on the input curved object surface are matched against those of each object model constructed in the learning phase, and the input object is finally classified according to

the match measures computed in the matching process.

Compared with the previously-mentioned approaches, the proposed approach at least has the following advantages.

(1) Only a single view of each object is needed for recognizing an object. This reduces the recognition time of each object.
(2) The formulas derived for computing the camera parameters are analytic, making the parameter computation work faster, and on-line 3-D data acquisition possible. This contrasts with most approaches of the type of 3-D recognition by 3-D matching, which usually spend large amounts of time in 3-D data acquisition and transformation.
(3) Well-developed 2-D shape matching can be easily applied in the model matching step.
(4) Both the learning and recognition phases follow an identical procedure. This reduces the complexity of the proposed approach.
(5) Since not only silhouette shapes but also surface patterns are utilized in the recognition scheme, more features can be extracted and higher recognition rates can be achieved.

In the remainder of the paper, the principle of the proposed cylindrical object recognition system is first presented. The camera calibration and surface backprojection techniques are then described. Detailed discussions on the object learning and recognition procedures follow next. Experimental results and conclusions are presented finally.

2. PRINCIPLE OF PROPOSED APPROACH

In this study, it is desired to utilize object surface patterns as well as silhouette object shapes to recognize 3-D cylindrical objects. The reason is that a lot of commercial products, like cans wrapped with paper on their surfaces, are cylindrical in shape and have abundant gray-scale or color pattern information on their surfaces which can be utilized in recognition. It is also desired to recognize objects by single views. This will increase the applicability of the recognition scheme. To accomplish these goals, first the object surface patterns, which are deformed in the input image due to imaging transformation, must be reconstructed. For this, we employ a new camera calibration technique, which can be performed in an on-line fashion, followed by a surface backprojection technique. After the 2-D surface patterns are obtained, object recognition is performed using a 2-D pattern matching method.

More specifically, a cylindrical object to be recognized is put on a flat surface within the field of view of a TV camera which is fixed at a known height. The position of the object with respect to the camera can be arbitrary. Image processing techniques are then applied to extract the boundary and normal lines of the object surface in the image (see Figure 1 for illustration). The equations of the two normal lines and the bottom planar curve are used to compute the camera parameters. The principle behind the proposed camera calibration process is that the two normal lines and the bottom planar curve contain abundant information about the position and the orientation of the camera (i.e., about the camera parameters). Analytical solutions for the camera parameters have been derived in this study for fast computation and this speeds up on-line object recognition.

After the camera parameters are computed, a surface backprojection technique is then employed to compute the 3-D coordinates of the pattern points on each surface of the cylindrical object. From these 3-D data, 2-D surface patterns are then reconstructed. Based on the reconstruction results, the learning phase and the recognition phase can be proceeded easily.

3. PROPOSED CAMERA CALIBRATION TECHNIQUE

3.1. Coordinate Transformations

Figure 1 shows the global coordinate system associated with a cylinder, which is used in this study. Let lines L_1 and L_2 denote the two normal lines. The values h and R are the height and

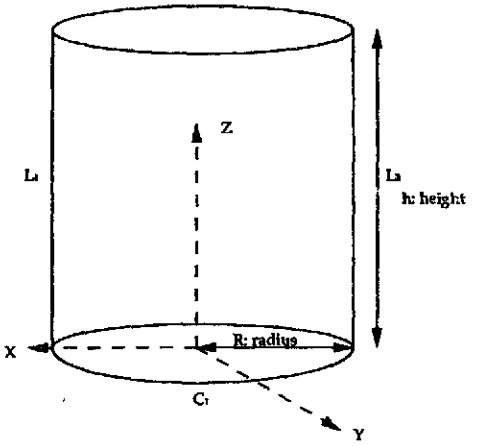

Figure 1. The global coordinate system attached on a cylinder to be recognized, where L_1 and L_2 are the normal lines and C_1 is the bottom curve (a circle).

the radius of the cylinder, respectively. In the right-handed global system, the Z-axis and the X-Y plane are chosen to be parallel to the normal lines and the bottom planar curve, respectively. And on the bottom planar curve which is an ellipse in the image, the center of the ellipse, the major axis, and the minor axis are selected to be the origin, the X-axis, and the Y-axis of the global system, respectively.

The camera location with respect to the global coordinate system is represented by three position parameters X_c, Y_c, and Z_c and three orientation parameters φ, θ and δ, where φ, θ and δ are called the Eulerian angles [13], or the pan, tilt, and swing angles of the camera, respectively. In this study, it is assumed that the parameter Z_c (i.e., the camera height) is known in advance, and it is desired to solve the remaining five camera parameters in terms of the equation coefficients of the two normal lines and those of the bottom planar curve.

Let (x, y, z) and (u, v, w) represent the coordinates of a point P in the 3-D space with respect to the global coordinate system and with respect to the camera coordinate system, respectively. Then, the coordinate transformation from (x, y, z) and (u, v, w) can be described as follows [14]:

$$(u, v, w, 1) = (x, y, z, 1)\ \mathbf{T}(X_c, Y_c, Z_c)\ \mathbf{R}_z(\varphi)\ \mathbf{R}_x(\theta)\ \mathbf{R}_z(\delta)\ \mathbf{T}_{r1} \tag{1}$$

$$= (x, y, z, 1)\ \mathbf{M}, \tag{2}$$

where

$$\mathbf{T}(X_c, Y_c, Z_c) = \begin{bmatrix} 1 & 0 & 0 & 0 \\ 0 & 1 & 0 & 0 \\ 0 & 0 & 1 & 0 \\ -X_c & -Y_c & -Z_c & 1 \end{bmatrix}, \tag{3}$$

$$\mathbf{R}_z(\varphi) = \begin{bmatrix} \cos\varphi & -\sin\varphi & 0 & 0 \\ \sin\varphi & \cos\varphi & 0 & 0 \\ 0 & 0 & 1 & 0 \\ 0 & 0 & 0 & 1 \end{bmatrix}, \tag{4}$$

$$\mathbf{R}_x(\theta) = \begin{bmatrix} 1 & 0 & 0 & 0 \\ 0 & \cos\theta & -\sin\theta & 0 \\ 0 & \sin\theta & \cos\theta & 0 \\ 0 & 0 & 0 & 1 \end{bmatrix}, \tag{5}$$

$$\mathbf{R}_z(\delta) = \begin{bmatrix} \cos\delta & -\sin\delta & 0 & 0 \\ \sin\delta & \cos\delta & 0 & 0 \\ 0 & 0 & 1 & 0 \\ 0 & 0 & 0 & 1 \end{bmatrix}, \tag{6}$$

$$\mathbf{T}_{r1} = \begin{bmatrix} 1 & 0 & 0 & 0 \\ 0 & 1 & 0 & 0 \\ 0 & 0 & -1 & 0 \\ 0 & 0 & 0 & 1 \end{bmatrix}, \qquad \text{and} \tag{7}$$

$$\mathbf{M} = \mathbf{T}(X_c, Y_c, Z_c)\ \mathbf{R}_z(\varphi)\ \mathbf{R}_x(\theta)\ \mathbf{R}_z(\delta)\ \mathbf{T}_{r1}, \tag{8}$$

with

$$\mathbf{M} = \begin{bmatrix} V_1 & V_2 & V_3 & 0 \\ V_4 & V_5 & V_6 & 0 \\ V_7 & V_8 & V_9 & 0 \\ O_1 & O_2 & O_3 & 1 \end{bmatrix}, \tag{9}$$

$$V_1 = \cos\varphi \cos\delta - \sin\varphi \cos\theta \sin\delta, \tag{10}$$

$$V_2 = -\cos\varphi \sin\delta - \sin\varphi \cos\theta \cos\delta, \tag{11}$$

$$V_3 = \sin\varphi \sin\theta, \tag{12}$$

$$V_4 = \sin\varphi \cos\delta + \cos\varphi \cos\theta \sin\delta, \tag{13}$$

$$V_5 = -\sin\varphi \sin\delta + \cos\varphi \cos\theta \cos\delta, \tag{14}$$

$$V_6 = \cos\varphi \sin\theta, \tag{15}$$

$$V_7 = \sin\theta \sin\delta, \tag{16}$$

$$V_8 = \sin\theta \cos\delta, \tag{17}$$

$$V_9 = -\cos\theta, \tag{18}$$

$$O_1 = -X_c V_1 - Y_c V_4 - Z_c V_7, \tag{19}$$

$$O_2 = -X_c V_2 - Y_c V_5 - Z_c V_8, \tag{20}$$

$$O_3 = -X_c V_3 - Y_c V_6 - Z_c V_9. \tag{21}$$

Note that all the elements V_i of matrix $\mathbf{M}$ in the above equations are in terms of φ, θ and δ only. V_i will be called the global orientation parameters, while O_i the global position parameters.

3.2. Proposed Method for Camera Calibration

Let P′ be the projection of Point P described in Section 3.1 in the image plane with image coordinates (U, V). Then, according to imaging geometry [15], we have

$$U = \frac{f u}{w}, \tag{22}$$

$$V = \frac{f v}{w}, \tag{23}$$

where f is the camera focal length and (u, v, w) are the coordinates of P in the camera coordinate system.

Let the equations of the corresponding projections of the two normal lines L_1 and L_2 in the image plane be

$$\begin{aligned} L_1' &: \quad u + b_1 v + c_1 = 0, \\ L_2' &: \quad u + b_2 v + c_2 = 0, \end{aligned} \tag{24}$$

and the equation of the bottom planar curve C_1 in the global coordinate system be

$$A x^2 + B x y + C y^2 + D x + E y + F = 0, \qquad \text{and } z = 0. \tag{25}$$

Also, let the equation of the projection C_1' of C_1 in the image plane be

$$A' u^2 + B' u v + C' v^2 + D' u + E' v + F' = 0. \tag{26}$$

Then, by comparing the corresponding coefficients A through F and A' through F', the global orientation parameters $V_1, V_2, \ldots, V_9$ and the global position parameters O_1, O_2, and O_3 can be solved as follows (the details are omitted) [16].

From the information of the two normal lines, the global orientation parameters V_7, V_8, and V_9 can be derived to be as follows:

$$V_7 = -\frac{1}{\sqrt{(1 + v_8^2 + v_9^2)}}, \tag{27}$$

$$V_8 = v_8 V_7, \tag{28}$$

$$V_9 = v_9 V_7, \tag{29}$$

where

$$v_8 = \frac{c_1 - c_2}{b_1 c_2 - b_2 c_1}, \tag{30}$$

$$v_9 = \frac{f b_2 - f b_1}{b_1 c_2 - b_2 c_1}. \tag{31}$$

And from the information of the bottom planar curve, the global orientation parameters V_1, V_2, and V_3 can be derived as follows:

$$V_1 = -\frac{1}{\sqrt{(1 + v_2^2 + v_3^2)}}, \tag{32}$$

$$V_2 = v_2 V_1, \tag{33}$$

$$V_3 = v_3 V_1, \tag{34}$$

where

$$v_2 = -\frac{G_3 + \sqrt{G_3^2 - 4G_1 G_2}}{2G_2}, \tag{35}$$

$$v_3 = \frac{-V_7 - v_2 V_8}{V_9}, \tag{36}$$

with

$$G_1 = H_{11} - H_{21}, \tag{37}$$

$$G_2 = H_{12} - H_{22}, \tag{38}$$

$$G_3 = H_{13} - H_{23}, \tag{39}$$

where

$$\begin{aligned} H_{ij} &= h_2(v_{j,3i-2}, v_{j,3i-1}, v_{j,3i}), && \text{for } i = 1,2, \quad j = 1,2, \\ &= \bar{h}_2(v_{1,3i-2}, v_{1,3i-1}, v_{1,3i}, v_{2,3i-1}, v_{2,3i}), && \text{for } i = 1,2, \quad j = 3, \end{aligned} \tag{40}$$

with

$$h_2(u, v, w) = A' f^2 u^2 + B' f^2 u v + C' f^2 v^2 + D' f u w + E' f v w + F' w^2, \tag{41}$$

$$\begin{aligned} \bar{h}_2(u_1, v_1, w_1, u_2, v_2, w_2) = {} & 2A' f^2 u_1 u_2 + B' f^2 (u_1 v_2 + u_2 v_1) + 2C' f^2 v_1 v_2 \\ & + D' f^2 (u_1 w_2 + u_2 w_1) + E' f (v_1 w_2 + v_2 w_1) \\ & + 2F' w_1 w_2. \end{aligned} \tag{42}$$

And using the orthonormal constraints among $V_1, V_2, \ldots, V_9$, the global orientation parameters V_4, V_5, and V_6 can be solved to be as follows:

$$V_4 = V_9 V_2 - V_8 V_3, \tag{43}$$
$$V_5 = V_7 V_3 - V_9 V_1, \tag{44}$$
$$V_6 = V_8 V_1 - V_7 V_2. \tag{45}$$

Now for this study, since the value of Z_c is known in advance, i.e., since the distance between the origin point O of the global coordinate system and the origin point C of the camera coordinate system, is given, the global position parameters O_1, O_2, and O_3 can be solved to be as follows:

$$O_1 = -X_c V_1 - Y_c V_4 - Z_c V_7, \tag{46}$$
$$O_2 = -X_c V_2 - Y_c V_5 - Z_c V_8, \tag{47}$$
$$O_3 = -X_c V_3 - Y_c V_6 - Z_c V_9, \tag{48}$$

$$O_1 = e_{13} O_3 + e_{14}, \tag{49}$$
$$O_2 = e_{23} O_3 + e_{24}, \tag{50}$$

with

$$\left.\begin{aligned} e_{1j} &= \frac{E_{1j} E_{22} - E_{12} E_{2j}}{E_{11} E_{22} - E_{12} E_{21}}, \\ E_{2j} &= \frac{E_{11} E_{2j} - E_{1j} E_{2j}}{E_{11} E_{22} - E_{12} E_{21}}, \end{aligned}\right\} \quad j = 3, 4, \tag{51}$$

where

$$\begin{aligned} (E_{11}, E_{12}) &= (2A' f^2 V_1 + B' f^2 V_2 + D' f V_3,\ B' f^2 V_1 + 2C' f^2 V_2 + E' f V_3), \\ (E_{13}, E_{14}) &= \left(-D' f V_1 - E' f V_2 - 2F' V_3,\ \frac{D * C^*}{C}\right), \\ (E_{21}, E_{22}) &= (2A' f^2 V_4 + B' f^2 V_5 + D' f V_6,\ B' f^2 V_4 + 2C' f^2 V_5 + E' f V_6), \\ (E_{23}, E_{24}) &= \left(-D' f V_4 - E' f V_5 - 2F' V_6,\ \frac{E * C^*}{C}\right), \end{aligned} \tag{52}$$

with

$$C^* = h_2(V_4, V_5, V_6). \tag{53}$$

Substituting equations (49) and (50) into equations (46) and (47), respectively, and rearranging the results and equation (48), we get

$$X_c V_1 + Y_c V_4 + e_{13} O_3 = -Z_c V_7 - e_{14}, \tag{54}$$
$$X_c V_2 + Y_c V_5 + e_{23} O_3 = -Z_c V_8 - e_{24}, \tag{55}$$
$$X_c V_3 + Y_c V_6 + \quad O_3 = -Z_c V_9. \tag{56}$$

Accordingly, the parameter O_3, X_c, and Y_c can be solved to be as follows:

$$X_c = \frac{\begin{vmatrix} -Z_c V_7 - e_{14} & V_4 & e_{13} \\ -Z_c V_8 - e_{24} & V_5 & e_{23} \\ -Z_c V_9 & V_6 & 1 \end{vmatrix}}{\begin{vmatrix} V_1 & V_4 & e_{13} \\ V_2 & V_5 & e_{23} \\ V_3 & V_6 & 1 \end{vmatrix}}, \tag{57}$$

$$Y_c = \frac{\begin{vmatrix} V_1 & -Z_c V_7 - e_{14} & e_{13} \\ V_2 & -Z_c V_8 - e_{24} & e_{23} \\ V_3 & -Z_c V_9 & 1 \end{vmatrix}}{\begin{vmatrix} V_1 & V_4 & e_{13} \\ V_2 & V_5 & e_{23} \\ V_3 & V_6 & 1 \end{vmatrix}}, \tag{58}$$

$$O_3 = \frac{\begin{vmatrix} V_1 & V_4 & -Z_c V_7 - e_{14} \\ V_2 & V_5 & -Z_c V_8 - e_{24} \\ V_3 & V_6 & -Z_c V_9 \end{vmatrix}}{\begin{vmatrix} V_1 & V_4 & e_{13} \\ V_2 & V_5 & e_{23} \\ V_3 & V_6 & 1 \end{vmatrix}}. \tag{59}$$

The other two position parameters O_1 and O_2 can be solved using equations (49) and (50), respectively.

After the global orientation parameters and the global position parameters are solved, the camera orientation parameters φ, θ, and δ can be solved as follows:

$$\varphi = \tan^{-1}\left(-\frac{V_3}{V_6}\right), \tag{60}$$

$$\theta = \cos^{-1}(-V_9), \tag{61}$$

$$\delta = \tan^{-1}\left(\frac{V_7}{V_8}\right). \tag{62}$$

In the case of the proposed approach, the bottom planar curve is a circle, so $A = C = 1$, $B = D = E = 0$, $F = -R^2$. After substituting these values into the equations containing A through F, respectively, the camera parameters can be solved. After the camera parameters are computed, by comparing the coefficients of F and F' in equations (25) and (26), we can get the following equation:

$$A_0 O_3^2 + B_0 O_3 + C_0 = -R^2 C^*,$$

from which the radius R can be derived to be

$$R = \sqrt{\frac{-1}{C^*}(A_0 O_3^2 + B_0 O_3 + C_0)} \tag{63}$$

where

$$(A_0, B_0, C_0) = (h_2(e_{13}, e_{23}, 1), \bar{h}_2(e_{13}, e_{23}, 1, e_{14}, e_{24}, 0), h_2(e_{14}, e_{24}, 0)). \tag{64}$$

The height of the cylinder can also be determined, which will be discussed later in the next section. Hence, when the value of Z_c is given, the camera orientation parameters φ, θ, and δ and the camera position parameter X_c, Y_c, the radius parameter R, and the height parameter h can all be solved. Cylindrical Objects of different radii and heights can thus be recognized.

4. METHOD FOR RECONSTRUCTING SURFACE PATCH PATTERNS USING BACKPROJECTION TECHNIQUE

Once the camera parameters are solved, we can reconstruct the pixel data of the surface patterns using a surface backprojection technique. In Figure 2, let the coordinates of any point P in the image plane be (a, b). Then its coordinates in the camera coordinate system are (a, b, f). The line L_{bk} passing through the origin C of the camera coordinate system and point P is called the backprojection line of P. By the principle of backprojection [17], the coordinates of any point P′ on the backprojection line L_{bk} can be specified by (at, bt, ft) with t as a free variable. Let (x, y, z) be the desired corresponding coordinates in the global coordinate system. Then, using (2), we get

$$(at, bt, ft, 1) = (x, y, z, 1)\begin{bmatrix} V_1 & V_2 & V_3 & 0 \\ V_4 & V_5 & V_6 & 0 \\ V_7 & V_8 & V_9 & 0 \\ O_1 & O_2 & O_3 & 1 \end{bmatrix}, \tag{65}$$

from which we can derive the following three equations (the details are omitted):

$$x = \frac{m_2}{m_1}t - \frac{m_5}{m_1}, \tag{66}$$

$$y = \frac{m_3}{m_1}t - \frac{m_6}{m_1}, \tag{67}$$

$$z = \frac{m_4}{m_1}t - \frac{m_7}{m_1}, \tag{68}$$

where

$$m_1 = \begin{vmatrix} V_1 & V_2 & V_3 \\ V_4 & V_5 & V_6 \\ V_7 & V_8 & V_9 \end{vmatrix}, \quad m_2 = \begin{vmatrix} a & V_2 & V_3 \\ b & V_5 & V_6 \\ f & V_8 & V_9 \end{vmatrix}, \quad m_3 = \begin{vmatrix} V_1 & a & V_3 \\ V_2 & b & V_6 \\ V_3 & f & V_9 \end{vmatrix}, \quad m_4 = \begin{vmatrix} V_1 & V_3 & a \\ V_2 & V_6 & b \\ V_3 & V_9 & f \end{vmatrix},$$

$$m_5 = \begin{vmatrix} O_1 & V_2 & V_3 \\ O_2 & V_5 & V_6 \\ O_3 & V_8 & V_9 \end{vmatrix}, \quad m_6 = \begin{vmatrix} V_1 & O_1 & V_3 \\ V_2 & O_2 & V_6 \\ V_3 & O_3 & V_9 \end{vmatrix}, \quad m_7 = \begin{vmatrix} V_1 & V_3 & O_1 \\ V_2 & V_6 & O_2 \\ V_3 & V_9 & O_3 \end{vmatrix}. \tag{69}$$

From the above equations, the free variable t remains unsolved. As can be seen from Figure 3, any point P that lies on the surface of the cylinder and can be seen in the image must lie on either of the two surface patches, i.e., either on Patch 1 or on Patch 2.

Assume that Point P with global coordinates (x, y, z) lies on Patch 1. Then $x^2 + y^2 = R^2$, $y > 0$ and $z \leq 0$. From the constraint $x^2 + y^2 = R^2$, the free parameter t can be solved (the details omitted) to be

$$t = \frac{(m_x m_5 + m_3 m_6) \pm \sqrt{(m_x m_5 + m_3 m_6)^2 - (m_2^2 + m_3^2)(m_5^2 + m_6^2 - m_1^2 R^2)}}{(m_2^2 + m_3^2)}. \tag{70}$$

After substituting the value of t into equations (66)–(68) to get the values of x, y, and z, we can check if $y > 0$ and $z \leq 0$ are satisfied. If not, then Point P must lie on Patch 2 and so is ignored. By this process, the free variable t can be solved for each Point P lying on Patch 1 of the cylinder, and the 3-D coordinates (x, y, z) of Point P′ in the global coordinate system are also determined. In the meantime, the height h of the cylinder can be determined by the following procedure.

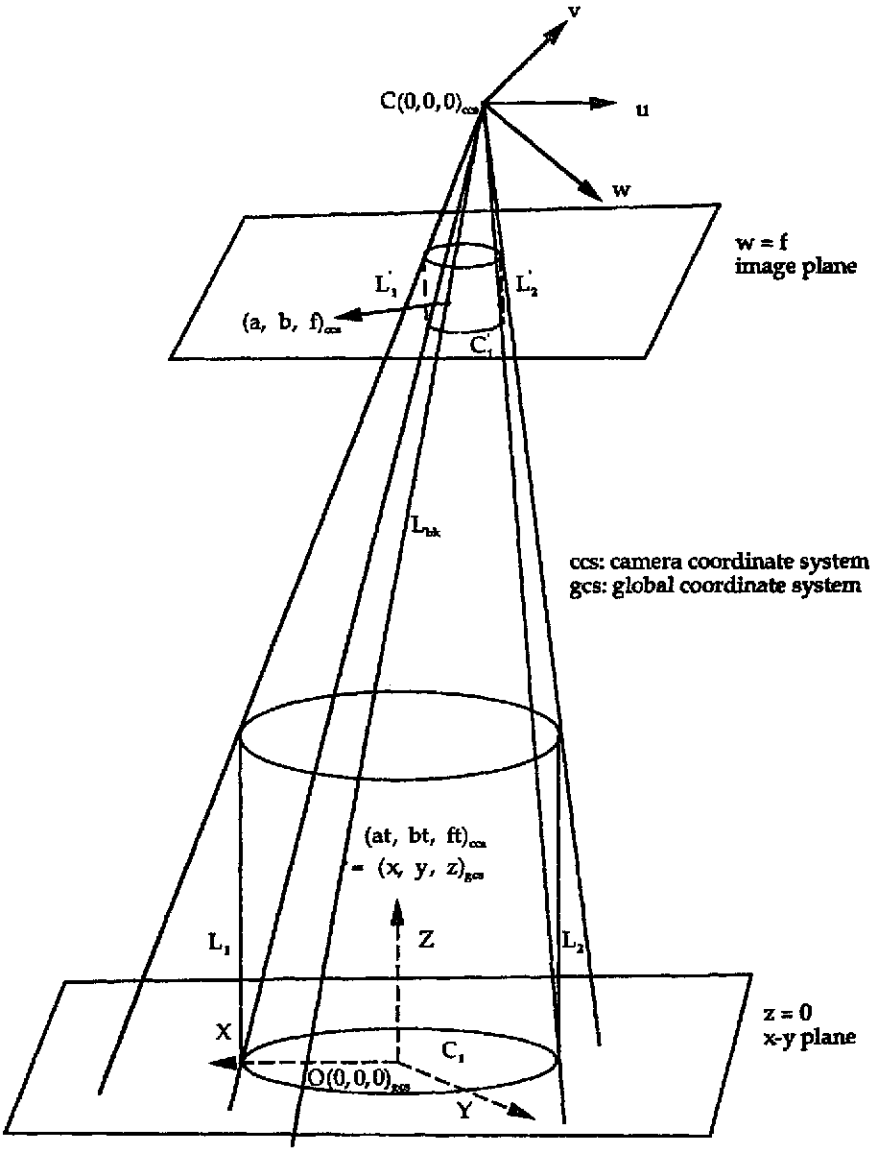

Figure 2. Illustration of the backprojection procedure.

First, substitute $a = u_1$ (or u_2), $b = v_1$ (or v_2) into equations (68) and (69), respectively. Then, solve (68), (69), and the equation of $z = h$ simultaneously. This results in

$$h = \frac{m_4}{m_1} t - \frac{m_7}{m_1}, \tag{71}$$

where t is described by (70).

After the 3-D coordinates of all points are determined, the points have also been grouped according to which surface patch they lie on. Since in most cases only Patch 1 contains pattern information, only the pattern on Patch 1 is reconstructed in this study. As shown in Figure 4, the reconstructed P-Q plane is established from the X-Y-Z global coordinate system. The coordinate of the P-axis is defined to be the length of the arc (seen from the top view) between the X-axis and Point A (see Figures 4a and 4b) and the coordinate of the Q-axis is the z-coordinate of the 3-D coordinates (x, y, z). The following procedure is employed in this study to reconstruct the pattern on Patch 1.

Let A be a point on Surface patch 1 with 3-D coordinates (x, y, z), and A_{top} denote the point corresponding to A as seen from the top of the cylinder (see Figure 4b). If $x > 0$, $y > 0$, then

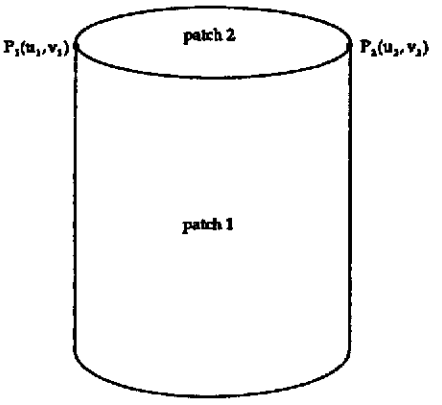

Figure 3. The Points P_1, P_2, and two surface patches on a cylinder as seen in an image.

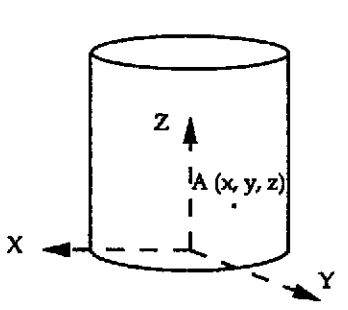

(a) The 3-D coordinate of a Point A on a cylinder.

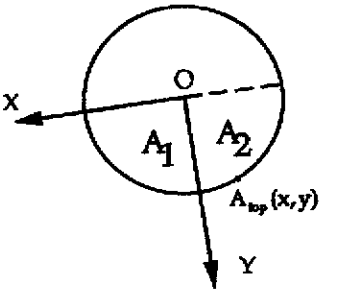

(b) The top view of the cylinder where A_{top} corresponds to A in (a).

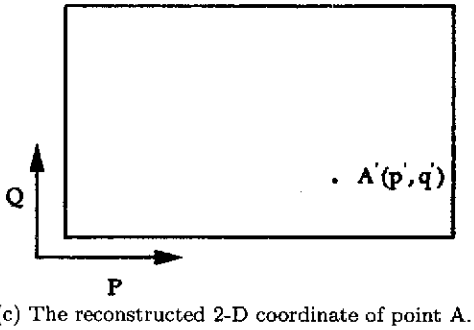

(c) The reconstructed 2-D coordinate of point A.

Figure 4. The reconstruction of 3-D points on the cylinder.

A_{top} lies in the area A_1, and the reconstructed coordinates (p', q') for A in the P-Q plane can be easily derived to be

$$p' = R\left(\tan^{-1}\frac{y}{x}\right) \quad \text{and} \quad q' = z. \tag{72}$$

Otherwise, A_{top} lies in the area A_2, and (p', q') can be derived to be

$$p' = R\left(\pi - \tan^{-1}\frac{y}{|x|}\right) \quad \text{and} \quad q' = z. \tag{73}$$

The binary values of the surface patch points form a 2-D point pattern, which can then be used for object recognition, as described in the next section.

5. LEARNING AND RECOGNITION PHASES

5.1. Learning Phase

Figure 5 shows the flowchart of the learning phase. First, if there is any model to be built, then an appropriate view of the model object is taken. Relevant image operations (thresholding, edge detection, thinning, and curve fitting [18]) are then applied to the image to get the line boundary and the points of the surface of the cylinder. The coefficients of the equations of the normal lines (L_1 and L_2) and the bottom plane curve are also found, and the camera parameters and the radius and height of the cylinder are computed. The surface patch patterns of the cylinder then are reconstructed using the surface backprojection technique.

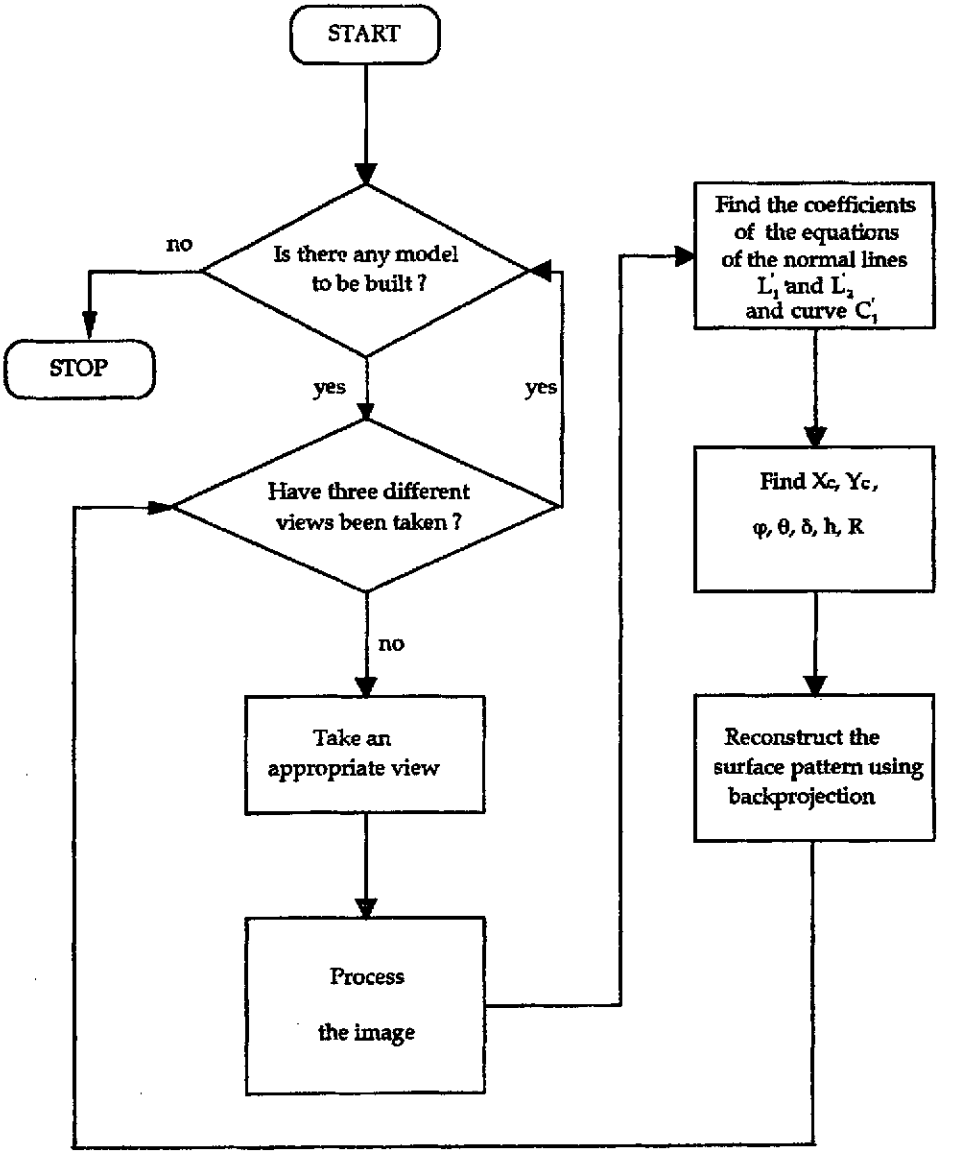

Figure 5. Flowchart of the learning phase.

5.2. Recognition Phase

Figure 6 shows the flowchart of the recognition phase. It starts from the camera calibration procedure. That is, each time an object is to be recognized, the camera parameters are found out first. After the calibration step, the surface pattern is reconstructed accordingly. In the step

of matching, the computed radius and height of the cylinder are first used to reject inappropriate surface patterns in the object models. Then, a similarity value DWC (distance weighted correlation [15]) between the reconstructed surface pattern of the input object and that of each object model is computed to decide if the surface patch patterns match well. If the reconstructed surface pattern matches well with that of a certain object, say A, in the object model, then we conclude that the object to be recognized is Object A. Otherwise, we decide that the object is unknown. In this way, cylinder objects of different radii, heights, and surface patterns can be recognized.

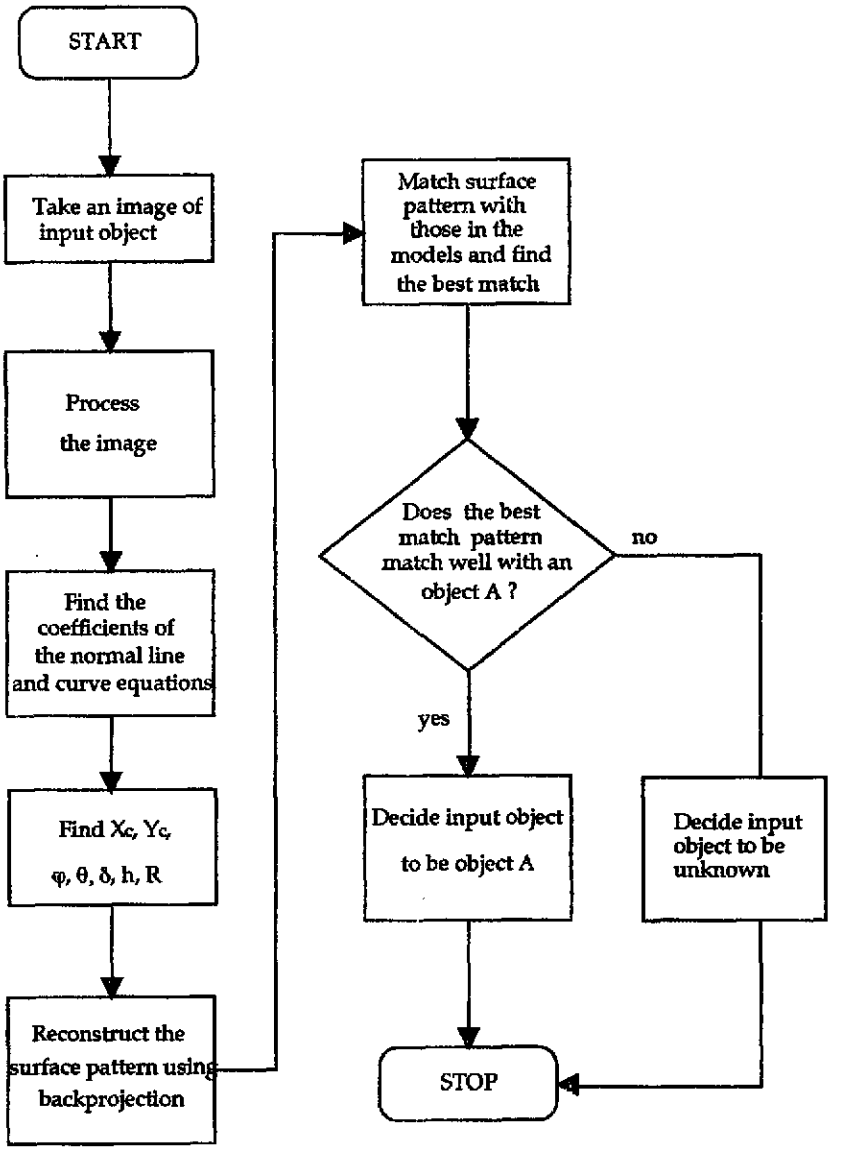

Figure 6. Flowchart of the recognition phase.

The partial shape matching method we employ in this study is the coarse-to-fine approach proposed by Rosenfeld and Vanderbrug [19], which is appropriate for matching point patterns.

6. EXPERIMENTAL RESULTS

Some experiments have been conducted on an IBM PC with an 80286 processor using a CCD TV camera. Figure 7 shows the diagram of the experimental environment. Once the environment

has been set up, the parameters Z_c and f are fixed. To compute the exact values of f and Z_c, a cylindrical object with known radius R_1 and height h_1 is used as a calibration object first. Then Z_c and f are estimated roughly. By using these rough values of Z_c and f and setting a reasonable search range (15%) around Z_c and f, the equations (63) and (71) are used to compute the radius and height (denoted as R_2 and h_2, respectively) of the cylindrical object iteratively until the difference between the pairs (R_1, h_1) and (R_2, h_2) is within some tolerance. The resulting values of Z_c and f then are taken as the exact values. Once the exact values of Z_c and f are obtained, any cylindrical object can be recognized accordingly as long as the environment remains unchanged.

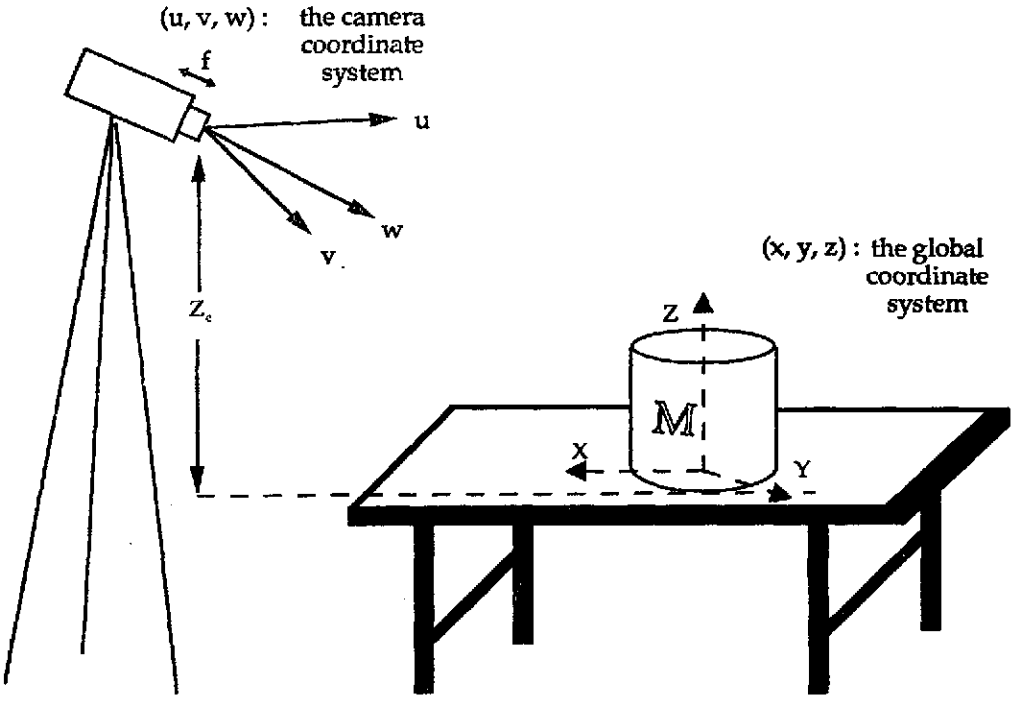

Figure 7. The diagram of the experimental environment where f is the focus length and Z_c is the camera height (the difference between the height of the camera lens center and that of the table).

To show the feasibility of the approach, three cylindrical objects were recognized. Cylindrical object 1 and Cylindrical object 2 were of the same height but of different radii. Cylindrical object 2 and Cylindrical object 3 were of the same height and radius. Since the proposed method can also compute the radius of the cylinder, Cylindrical object 1 can be discriminated immediately from Cylindrical objects 2 and 3. The surface patterns of the objects include numbers, English characters, and geometric patterns. Figures 8a–c are the results of processing the image of Cylindrical object 1 with a number pattern on its side surface. Figure 8d is the result of reconstructing the surface pattern of Cylindrical object 1. Due to possible errors in the image processing step, some distortion occurs on the boundary of the reconstructed surface pattern of the cylinder. But such distortion usually does not influence the result of the subsequent surface pattern matching process because the boundary, which is not essential information for object discrimination, was removed in our experiments before surface pattern matching. Similarly, Figures 9a–c and Figures 10a–c are the results of image processing of Cylindrical object 2 (with a character pattern) and Cylindrical object 3 (with a geometric shape pattern), respectively. Figure 9d and Figure 10d are the results of surface patch reconstruction for Cylindrical object 2 and Cylindrical object 3, respectively. Table 1 includes the results of the computed camera parameters and the radii and heights of the Cylindrical objects. From the table, we see that the errors of the computed cylinder radii and heights are less than 5%. Table 2 includes the results of the

similarity measures between the surface patterns of the objects to be recognized and those of the object models. The surface pattern of each cylindrical object is assigned correctly to that of the model. As the results show, the three cylindrical objects of different surface patterns were all recognized correctly. The recognition rate is over 90%.

(a) Input image of Cylindrical object 1.

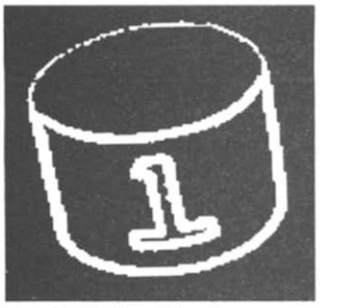

(b) Result of edge detection.

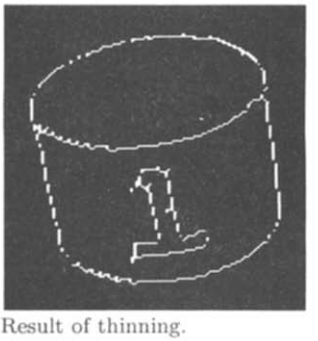

(c) Result of thinning.

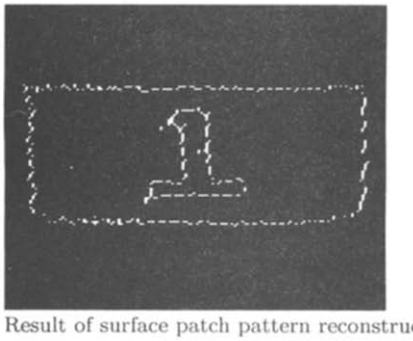

(d) Result of surface patch pattern reconstruction.

Figure 8. Experimental results for Cylindrical object 1 with a number pattern on its surface patch.

(a) Input image of Cylindrical object 2.

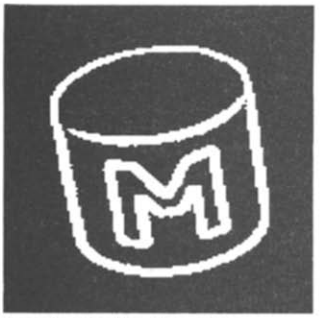

(b) Result of edge detection.

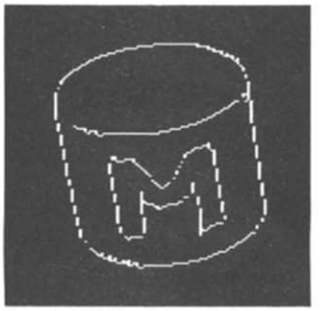

(c) Result of thinning.

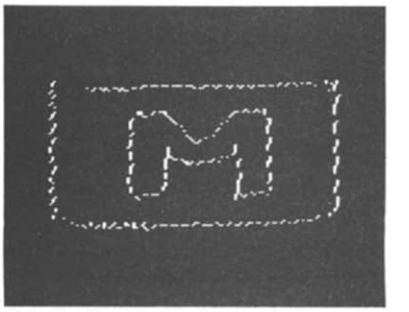

(d) Result of surface patch pattern reconstruction.

Figure 9. Experimental results for Cylindrical object 2 with a character pattern on its surface patch.

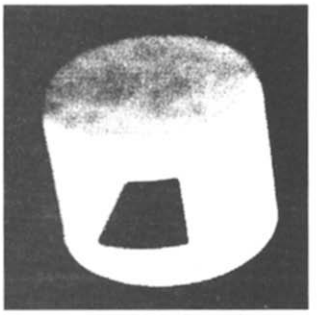

(a) Input image of Cuboidal object 3.

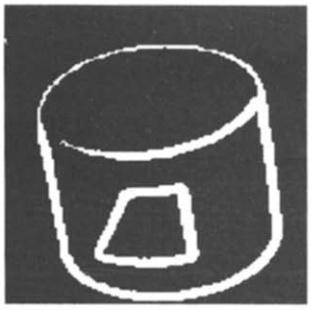

(b) Result of edge detection.

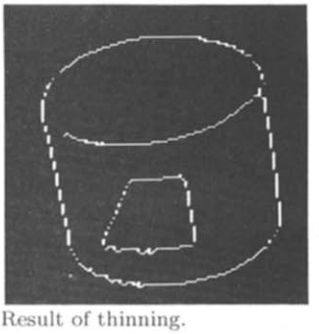

(c) Result of thinning.

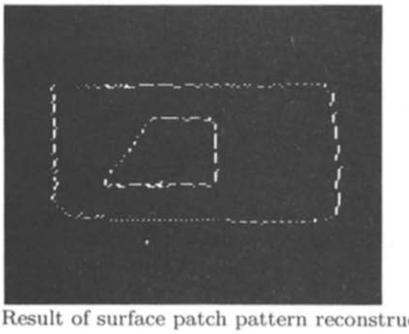

(d) Result of surface patch pattern reconstruction.

Figure 10. Experimental results for Cylindrical object 3 with a character pattern on its surface patch.

Table 1. Result of computed camera parameters and dimensions of the Cylindrical objects (the actual values of R and h for Object 1 are 3.5 and 5.0, respectively, while those of R and h for Object 2 and Object 3 are 3.0 and 5.0, respectively. And the numbers in the parentheses are the error percents of the size).

	Object 1	Object 2	Object 3
f (pixel)	1011	1011	1011
X_c (cm)	−29.59	−10.23	15.49
Y_c (cm)	36.3	45.63	30.26
Z_c (cm)	37.1	37.1	37.1
φ (°)	40.10	13.15	−26.5
θ (°)	52.70	51.60	46.54
δ (°)	−10.08	−10.05	−8.92
R (cm)	3.61(3.14)	3.03(1.0)	3.11(3.7)
h (cm)	4.92(1.6)	5.10(2.0)	4.93(1.4)

Table 2. Result of computed similarity measures between the surface patterns of the recognized objects and those of the object models ("*" means that the measure need not be computed).

	Object 1	Object 2	Object 3
Model 1	0.61	*	*
Model 2	*	0.59	0.08
Model 3	*	0.12	0.67

7. CONCLUSIONS

A new approach to 3-D object recognition has been proposed, and some experimental results have been shown to prove the feasibility of the approach. The approach consists of the steps of on-line camera calibration, backprojection for object surface reconstruction, and surface pattern

matching for object recognition. Cylindrical objects in arbitrary positions can be recognized by single camera views. This increases the flexibility of the proposed approach. The analytic solutions of the camera parameters speed up the camera calibration process. The use of the computed cylinder radius, height, and surface pattern improves the discrimination capability of the proposed approach.

REFERENCES

1. R.T. Chin and C.R. Dyer, Model-based recognition in robot vision, *Computing Surveys* **18** (1), 67–108 (1986).
2. J. Besl and R.C. Jain, Three-dimensional object recognition, *Computing Surveys* **17** (1), 75–145 (1985).
3. T.M. Silberberg, L. Davis, and D. Harwood, An iterative Hough procedure for three-dimensional object recognition, *Pattern Recognition* **17** (6), 621–629 (1984).
4. Y.F. Wang, M.J. Maggee, and J.K. Aggarwal, Matching three-dimensional objects using silhouette, *IEEE Trans. Pattern Analysis and Machine Intelligence* **6** (4), 513–518 (1984).
5. T.P. Wallace and P.A. Wintz, An efficient three-dimensional aircraft recognition algorithm using normalized Fourier descriptor, *Computer Vision, Graphics, and Image Processing* **13**, 96–126 (1980).
6. S.A. Dudani, K.J. Breeding, and R.B. McGhee, Aircraft identification by moment invariants, *IEEE Trans. Computers* **C-26** (1), 395–412 (1977).
7. L.T. Watson and L.G. Shapiro, Identification of spaces from two-dimensional perspective views, *IEEE Trans. Pattern Analysis and Machine Intelligence* **4** (5), 469–475 (1982).
8. C.H. Liu and W.H. Tsai, 3-D curved object recognition from multiple 2-D camera views, *Computer Vision, Graphics, and Image Processing* **50**, 177–187 (1990).
9. M.C. Yang and W.H. Tsai, Recognition of single 3-D curved objects using 2-D cross-sectional slice shapes, *Image and Vision Computing* **7** (3), 210–216 (1989).
10. A.K.C. Wong, S.W. Lu, and M. Rioux, Recognition and shape synthesis of 3-D objects based on attributed hypergraph, *IEEE Trans. Pattern Analysis and Machine Intelligence* **11** (3), 279–290 (1989).
11. M. Oshima and Y. Shirai, Object recognition using three-dimensional information, *IEEE Trans. Pattern Analysis and Machine Intelligence* **PAMI-5** (4), 353–361 (1983).
12. R.A. Brooks, Model-based three-dimensional interpretations of two-dimensional images, *IEEE Trans. Pattern Analysis and Machine Intelligence* **PAMI-5** (2), 140–150 (1983).
13. K.S. Fu, R.C. Gonzalez, and C.S.G. Lee, *Robotics: Control, Sensing, Vision and Intelligence*, McGraw-Hill, New York, (1987).
14. J.D. Foley and A. Van Dam, *Fundamentals of Interactive Computer Graphics*, Addison-Welsley, Reading, MA, (1982).
15. T.J. Fan and W.H. Tsai, Automatic Chinese seal identification, *Computer Vision, Graphics and Image Processing* **25**, 311–330 (1984).
16. S.Y. Chen and W.H. Tsai, Robot rocation using surface patch of curved objects, *Int. J. Robotics and Automation* **4**, 123–133 (1989).
17. H. Steven, *Computer Graphics*, McGraw-Hill, New York, (1978).
18. C.A. McPherson, and E.L. Hall, Curved surface representation for image recognition, *Proc. IEEE Conf. Pattern Recognition and Image Processing*, Las Vagas, Nevada, 363–369 (June, 1982).
19. A. Rosenfeld and J. Vanderbrug, Coarse-fine template matching, *IEEE Trans Systems, Man and Cybernetics* **SMC-7** (2), 104–107 (1977).